Journal of Energy Storage 68 (2023) 107771

Contents lists available at ScienceDirect

Journal of Energy Storage

journal homepage: www.elsevier.com/locate/est

Research papers

Effect of TPRD diameter and direction of release on hydrogen dispersion and jet fires in underground parking

V. Shentsov *, D. Cirrone, D. Makarov

Hydrogen Safety Engineering and Research Centre (HySAFER), Ulster University, Shore Road, Newtownabbey BT37 0QB, UK

ARTICLE INFO

Keywords:
Hydrogen safety
Unignited release
Jet fire
Mechanical ventilation
Underground parking
TPRD
CFD

ABSTRACT

The paper presents safety strategies to support choice of diameter and release direction for thermally activated pressure relief device (TPRD) onboard a hydrogen fuel cell electric vehicle. Analytical and numerical modelling campaigns were performed to study hazards of unignited and ignited hydrogen releases from a vehicle in a real underground parking. TPRD diameter to prevent flammable mixture formation during upward release was determined using similarity law for hydrogen concentration decay along jet centreline. Parametric CFD simulations studied effect of different TPRD diameter, release direction, vehicle distance from obstacles, ceiling height, influence of carpark ventilation on hydrogen hazards. Hazards of unignited releases were associated with the lower flammability limit of hydrogen-air clouds. For ignited releases the temperature threshold 70 °C was used as a no-harm criteria for assessment of thermal hazards to people and threshold 300 °C as a damage criteria for mechanical ventilation system following requirements of BS 7346-7-2013 standard for carpark ventilation. Recommendations on TPRD design were formulated to support safe integration of hydrogen-powered vehicles in the existing underground parking facilities and infrastructure.

1. Introduction

The development of safety strategies to prevent the formation of flammable hydrogen-air composition in underground traffic infrastructure and parking areas is of interest for safety and design engineers in connection with increasing number of fuel cell electric vehicles (FCEV) on public roads. In case of a hydrogen leak in an enclosure, it is recommended to have a ventilation system preventing accumulating of hydrogen concentration above 1 % vol. [1–3]. In the context of underground parking, the hydrogen release may originate from an accidentally triggered thermally activated pressure relief device (TPRD), which is a standard safety feature required for onboard storage of every FCEV. Requirements for mechanical ventilation installed in underground parking areas to control air quality and to counteract potential fire hazards are specified by corresponding regulations, codes and standards (RCS), e.g. BS 7346-7-2013 [4]. In the event of a fire, the BS 7346-7-2013 requires that a mechanical ventilation system shall clear the smoke produced by the fire to facilitate the occupants escape and the first responders' intervention and shall provide at least 10 Air Changes per Hour (ACH). This standard also states that "All fans intended to exhaust hot gases used within a car park ventilation system should be tested in accordance with BS EN 12101-3 to verify their suitability for operating at 300 °C for a period not less than 60 minutes (class F300)." Interaction of hydrogen releases from TPRD with mechanical ventilation in underground parking is a credible accident scenario. It is fundamental to assess whether potential unignited or ignited releases from a TPRD would lead to non-compliance of existing carpark mechanical ventilation with the requirements of current RCS for underground parking. Furthermore, it should be ensured that the hydrogen release from a TPRD would not present hazards to people obstructing their self-evacuation from the FCEV and preventing operations of fire and rescue services.

The effect of mechanical ventilation on hydrogen dispersion in closed spaces was examined in few numerical studies. In CFD study [5] hydrogen TPRD releases were simulated using FLACS in a private and large parking garage. Release flow rates started from 500 g/s taking into account blowdown, however, TPRD orifices were not specified and ventilation was absent, as the focus of the study was on comparison of hydrogen and methane blend i.e. hythane. The paper was mainly focused on the assessment of pressure effects rather on the TPRD choice. In 2013 Choi et al. [6] performed numerical simulations of hydrogen release from onboard storage in an underground parking with and

* Corresponding author.
E-mail addresses: v.shentsov@ulster.ac.uk (V. Shentsov), d.cirrone@ulster.ac.uk (D. Cirrone), dv.makarov@ulster.ac.uk (D. Makarov).

https://doi.org/10.1016/j.est.2023.107771
Received 22 March 2023; Received in revised form 15 May 2023; Accepted 18 May 2023
Available online 24 May 2023

without mechanical ventilation. The considered parking had dimensions $W \times L \times H = 18.0 \times 16.7 \times 2.3$ m. In simulations with ventilation the parking entrance was wide open, $W \times H = 5.0 \times 2.3$ m, with mechanical ventilator located on the floor centrally and air flow direction towards the parking exit. Ventilation rates of 20, 40 and 60 m^3/min were simulated, which corresponded to 1.7, 3.5 and 5.2 ACH. Hydrogen release was simulated vertically downward, with a release opening 5 × 5 cm, hydrogen velocity chosen to provide constant volume rate Q = 0.655 and 1.310 m^3/min. The authors observed that for the studied hydrogen flow rates the ventilation significantly affected the flammable cloud volume and practically eliminated it in both considered cases, which was attributed to a much larger ventilation rate than the hydrogen leakage and relatively low release velocity.

Matsuura et al. [7] examined numerically the effect of ventilation velocity in a scaled model of semi-open hallway ($L \times W \times H = 2.9 \times 0.74 \times 1.22$ m) aiming to devise a control system for the forced ventilation. One end of the hallway was completely open. A single hydrogen leak opening and a single roof vent had the same sizes, 0.15 × 0.30 m. Effect of vent location in the roof and hydrogen leak location in the floor for different release flow rates 1.18×10^{-4}–9.44×10^{-4} m^3/s, extraction fan rates 2.32×10^{-2}–6.97×10^{-1} m^3/s (32–958 ACH) and extraction fan operation pattern were studied. The authors demonstrated that under the investigated conditions the location of mechanical ventilation opening and ventilation rate had a significant effect on hydrogen distribution and propagation through the enclosure. The larger ventilation rates imposed strong inflow from the open end of the studied hallway, which overcame hydrogen plume buoyancy and prevented hydrogen from rising to the ceiling leading to its propagation along the floor.

Two engineering models were developed within HyIndoor project to aid ventilation design for indoor hydrogen installations. The passive ventilation model [8] assumes hydrogen accumulation from a steady-state release in a stratified layer under the enclosure ceiling. The approach was validated against 48 small-scale experiments with natural/passive ventilation performed by CEA [9] on helium release in a small scale enclosure of size $H \times W \times D = 1.26 \times 0.93 \times 0.93$ m with one vent located on a wall near the ceiling. The calculation procedure may also be adapted to find the volumetric flow rate of mechanical ventilation not to exceed the targeted maximum hydrogen concentration in the stratified layer for a given constant hydrogen release rate. The second model [10] is based on the perfect mixing equation and assumes uniform hydrogen distribution through the entire enclosure. The model allows calculating the forced ventilation flow rate not to exceed the targeted maximum hydrogen concentration for a given steady-state hydrogen release rate.

Solutions for both the passive ventilation model [8] and the forced ventilation perfect mixing model [10] are based on two strong assumptions: (1) perfect mixing in the stratified layer and perfect mixing in the entire enclosure respectively, (2) steady-state formulation corresponding to the constant hydrogen release rate. Violation of each of the approaches' assumptions leads to a decrease of the modelling results accuracy. Transient release of finite onboard storage inventory in a large enclosure, e.g. underground parking, is a real-life scenario leading to spatial and temporal distribution of hydrogen violating both above assumptions. Application of analytical models in this situation would not be justified and engineering solutions should employ more accurate technique like CFD analysis which is also applicable for the jet fires.

The recent study [11] within HyTunnel-CS project provides important insights into the effectiveness of mechanical ventilation systems during accidental hydrogen releases in confined spaces as underground garages. The experiments were conducted in a 40 ft. ISO container to find the mass flow rate limit and TPRD diameter limit that do not require a change in the ventilation system. The findings indicate a correlation between hydrogen concentration, mass flow rate, reservoir pressure, and ventilation rate. They concluded that the sufficiency of forced ventilation used today on hydrogen concentration was not conclusive, and it is recommended to keep the TPRD diameter small. In the case of unintended hydrogen releases in the parking garage, a ventilation rate of 10 ACH or higher is recommended to reduce the duration of the flammable cloud.

Overall, thorough assessment of the hazards associated with unintended hydrogen releases from a TPRD installed on a FCEV in an underground car parking are currently missing. This study aims at fulfilling this gap by means of numerical simulations of unignited and ignited hydrogen releases in a realistic underground car park scenario. This work has been performed within the framework of FCH JU funded project HyTunnel-CS on "Pre-normative research for safety of hydrogen driven vehicles and transport through tunnels and similar confined spaces" (https://hytunnel.net). The ambition of HyTunnel-CS project was to underpin the allowance of hydrogen-powered vehicles to enter the underground traffic infrastructure by closing the knowledge gaps and technological bottlenecks in the provision of safety associated to the use of such vehicles in underground transportation systems. This paper demonstrates how the safety strategies developed in HyTunnel-CS project [12] can be realised for underground car parking. Firstly, the research assesses the use of validated reduced tools available in literature for free unignited and ignited hydrogen jets for an underground car park scenario, defining the range of applicability of the reduced models. The scenarios involving complex geometries and hydrogen jets impinging on the ground are found to be outside the range of reduced models applicability. Thus, these scenarios are investigated using validated computational fluid dynamics (CFD) models. A systematic approach is employed to scrutinise the effect of a TPRD diameter and direction of an unignited and ignited hydrogen releases in the context of underground parking and/or traffic systems. Focus is posed on the investigation of the hydrogen release interaction with a typical for car parking mechanical ventilation system, compliance to current RCS requirements, facilitation of passengers' evacuation and rescue operations. The final aim is to propose suitable TPRD characteristics and safety strategies for the inherently safer introduction of FCEV in an underground car park without requiring modifications to the infrastructure.

2. Similarity law for assessment of upward releases

2.1. Safety strategy

The strategy for inherently safer FCEV underground parking is to eliminate the formation of a flammable cloud under the ceiling preventing the potential of its ignition and destructive deflagration. In the case of upward releases, the similarity law [13] can be used to calculate the TPRD diameter that would allow the jet decay below hydrogen lower flammability limit 4 % vol. before reaching the ceiling and prevent formation of flammable cloud. Hydrogen concentration decay along the centre-line of a free, unobstructed hydrogen jet can be described by fundamentally based and extensively validated for both expanded and underexpanded jets similarity law [13]:

$$\frac{C_{ax}}{C_N} = 5.4 \cdot \sqrt{\frac{\rho_N}{\rho_S}} \ \frac{D}{x}, \tag{1}$$

where x is the axial distance from the nozzle to the point of interest (m); D is the nozzle exit diameter (m); C_{ax} is a mass fraction of hydrogen in air at axial distance x; C_N is hydrogen mass fraction in the nozzle ($C_N = 1.0$ for pure hydrogen release); ρ_N is the density at the nozzle exit (kg/m^3); ρ_S is the ambient air density (kg/m^3). The similarity law was realised as one of the tools of e-Laboratory of hydrogen safety [14] developed within the project NET-Tools [15].

A simple safety strategy may be based on the minimisation of release opening to provide hydrogen concentration decay below the lower flammability limit (LFL) before the jet reaches the enclosure ceiling. Once hydrogen concentration under the ceiling is below LFL, i.e. 4 %

vol. hydrogen, then formation and built-up of flammable hydrogen-air cloud there is excluded. The similarity law can be reformulated to provide distance along the jet axis to the location where hydrogen mass fraction reaches the specified value:

$$x = \frac{5.4 \times D}{C_{ax}} \cdot \sqrt{\frac{\rho_N}{\rho_S}}, \tag{2}$$

where x is the vertical distance between the release orifice (i.e. TPRD location) and the ceiling (m), and $C_{ax} = 0.00288$ is the hydrogen mass fraction corresponding to the hydrogen LFL (4 % vol.).

2.2. Example of inherently safer TPRD diameter calculation

Example of finding TPRD diameter that would prevent formation of flammable hydrogen-air cloud under carpark ceiling is presented below. Let us consider a vehicle in underground parking with a ceiling height of 3.0 m. The vehicle onboard hydrogen storage pressure is 70 MPa. The storage is equipped with a TPRD that is installed at a height 0.5 m above the floor and vents vertically upward. The surrounding temperature is 288 K. The concentration on the jet axis at the ceiling should be below 4 % vol. (corresponding mass fraction is $C_{ax} = 0.00288$). For an unignited jet, the similarity law in Eq. (1) or the respective e-Laboratory [14] tool can be applied to calculate concentration on the jet axis. The location of the TPRD above the floor and the height of the ceiling must be taken into account for assessment. Procedure for calculations by hand [13]:

1. Calculate the pressure in the real nozzle exit as a function of the storage pressure:

$$P_N = \frac{P_R}{\left(\frac{\gamma+1}{2}\right)^{\frac{\gamma}{\gamma-1}}} = \frac{70000000\ Pa}{\left(\frac{1.4+1}{2}\right)^{\frac{1.4}{1.4-1}}} = 36979725\ \text{Pa}.$$

2. Calculate the Z factor using the Abel-Noble equation of state for real gas:

$$Z = 1 + \frac{b \cdot P_R}{R_{H2} \cdot T} = 1 + \frac{0.007691 \cdot 70000000\ Pa}{4124.24 \cdot 288\ K} = 1.4533.$$

3. Calculate density of hydrogen in the nozzle exit:

$$\rho_N = \frac{P_N}{Z \cdot R_{H2} \cdot T} = \frac{36979725\ Pa}{1.4533 \cdot 4124.24\ J/K/kmol \cdot 288\ K} = 21.4226\ \text{kg/m}^3.$$

4. Calculate the maximum nozzle diameter sufficient to exclude the formation of flammable cloud using:

$$D = \frac{x}{5.4} \frac{C_{ax}}{C_N} \sqrt{\frac{\rho_S}{\rho_N}} = \frac{2.5\ m}{5.4} \frac{0.00288}{1} \sqrt{\frac{1.205\ \text{kg/m3}}{21.4226\ \text{kg/m3}}} = 0.000316\ m$$
$$= 0.3\ \text{mm}.$$

This is a quite small diameter of TPRD and care should be taken that it is sufficient for hydrogen tank blowdown in a fire before the tank loses its load bearing ability and ruptures.

3. Dimensionless flame length correlation for ignited release

3.1. Safety strategy

The safety strategy for the ignited release can be assessed both in terms of harm to people and damage to the ventilation system. Temperature higher than 70 °C according to LaChance (2011) [16] is deemed to be unsafe for people and therefore calculation of temperature decay for the particular release is the way forward in assessment of the hazard distance. The no-harm condition 70 °C is reached at the distance 3.5 times larger than the flame length as shown in Fig. 1.

The damage to the ventilation system can be assessed using 300 °C temperature as the maximum limit that, according to the BS 7346-7-2013 [4], may be allowed at the ventilation intake for safe operation of the mechanical ventilation system in the event of a hydrogen jet fire. This is a conservative assessment as the duration of hydrogen jet fires will likely be shorter than 60 min.

The distance along the jet fire axis to the temperature limits of 70 °C and 300 °C can be calculated using the dimensionless correlation for flame length [17] implemented in the same e-Laboratory of hydrogen safety tools as described above. Fig. 1 shows the axial temperature distribution as a function of distance normalised by the flame length. It can be observed that the distance to the temperature of 300 °C (solid line in Fig. 1, coincides with the third degree burn harm to people) is equal to twice the flame length and it can be used as indication to know whether the combustion products having this temperature will enter the ventilation system or not.

3.2. Example of inherently safer TPRD diameter calculation

Let us consider the same example of FCEV in underground parking given in Section 2.2 and calculate the distance to 70 °C (no harm to people) and 300 °C (standard requirement for operation of mechanical ventilation in carpark) for the release with nozzle diameter equal to 0.3 mm and storage pressure of 700 bar. Calculation of the flame length using the dimensionless flame length correlation [17] or e-Laboratory [14] gives 1 m. Following axial distribution of temperature in Fig. 1, it can be found that distance to the limit of 300 °C is 2.0 m, whereas distance to "no-harm" threshold of 70 °C is 3.5 m. Considering that the release of hydrogen is located at 0.5 m above the ground, temperature limit 300 °C would be reached at the height 2.5 m and under the 3 m high ceiling the temperature should drop below 300 °C. Assuming that the ventilation duct is placed exactly above the release point, temperature of the hot combustion products at the entrance of the ventilation system would be comparable to the limit that can be considered as compliant with BS standards.

The considered above reduced models are based on assumption of a freely propagating jet and not applicable to releases directed downwards and impinging on the ground. More accurate assessment methods, like a CFD modelling presented below, shall be employed to find out the limits of TPRD diameters and downward release angles to ensure compliance to mechanical ventilation requirements and to provide safe self-evacuation of passengers in case of unintended ignited release.

4. Numerical study of downward release from TPRD

4.1. The CFD model details

4.1.1. Unignited release

In this study, we look into the example of a real underground car park in St. Martnes Latem (Gent, Belgium) [18]. The top view of the car park with dimensions is given in Fig. 2. The car park height is 3.0 m, the total parking area is 1115 m^2. Mechanical ventilation is organised using 18 evenly distributed vent openings having size 1 × 1 m each and located at the carpark ceiling. The onboard hydrogen storage with the volume of 62.4 l, initial storage pressure 70 MPa, initial temperature 288 K and several TPRD diameters were studied.

The transient problem formulation is considered to account for the blowdown of the storage tank. The mathematical model includes mass, momentum, energy and hydrogen mass fraction conservation equation. Effect of turbulence is modelled using realisable k-ε turbulence model [19]. The isometric view of calculation domain and numerical mesh are shown in Fig. 3. The calculation domain included the underground parking itself and part of the tunnel entrance (section BDEF in Fig. 2).

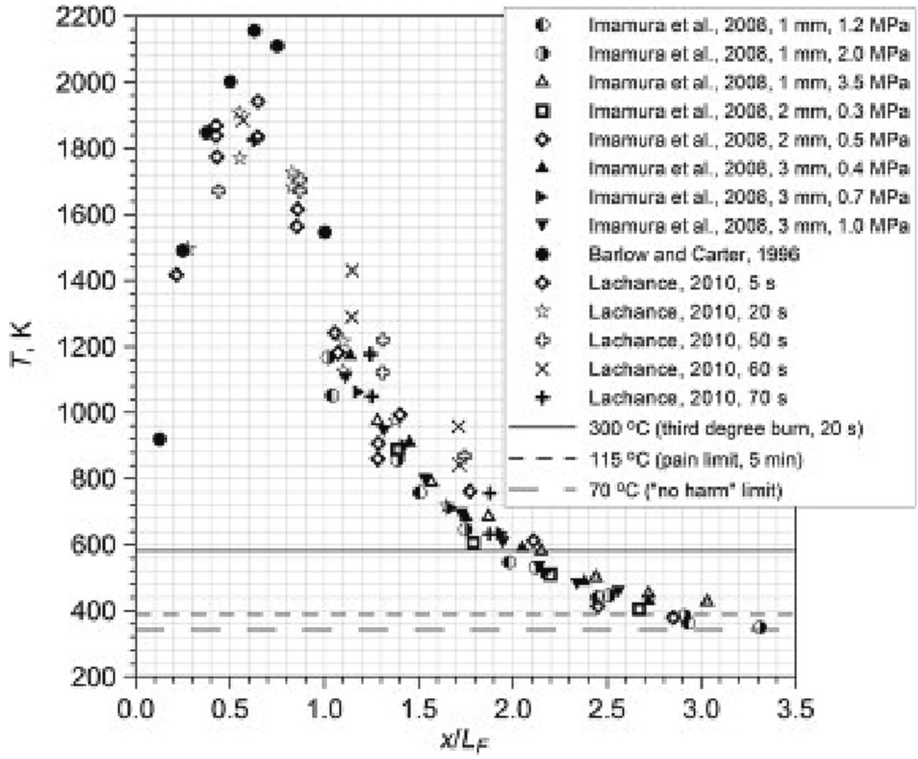

Fig. 1. Measured axial temperature as a function of distance normalised using flame length (symbols), and three criteria of jet fire harm to people (lines) [17].

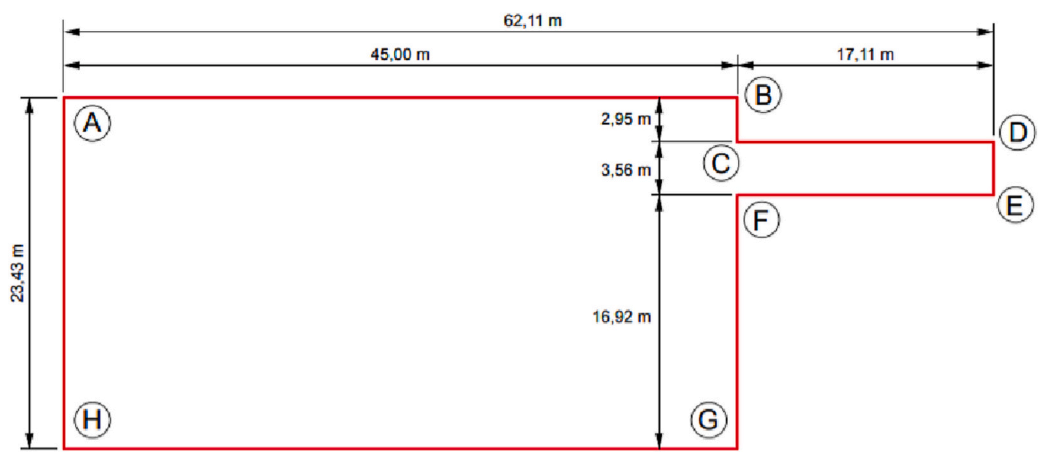

Fig. 2. Underground car park layout (St. Martnes Latem, Gent, Belgium) [18].

The numerical grids consisted of 440 k control volumes uniformly distributed inside the calculation domain and refined at the release zone. The numerical grids were constituted by polyhedral control volumes at the surfaces to better represent the impinging jets onto the ground, whereas they were hexahedral towards the core of the fluid. To improve gradient calculations, a polyhedral grid was used at the impinging zone as per previous study [20]. This was done in order to overcome the problem of gradient reconstruction that arises with other meshes. The control volume varied from 3.5 mm in the vicinity of the nozzle and up to 20 cm in the far field from the nozzle. Grid and time step independence studies have been previously performed in [21] for unignited releases, and the authors used the found criteria to formulate the problem in the current publication.

Initial conditions in the car park were ambient temperature equal to 288 K and ambient pressure of 101,325 Pa. The car park entrance, shown in Fig. 3 by the blue arrow, acts as an inlet for the fresh air and was modelled as a pressure boundary with gauge pressure equal to 0. The extraction ventilation openings, designated in Fig. 3 by red arrows, were arranged in evenly distributed over the ceiling extraction vents (18 vents, 1 × 1 m each) and simulated as outflow boundary with uniform velocity in the vent area. In simulations with mechanical ventilation the outflow velocity was specified in accordance with BS 7346-7:2013 [4] and accounted the car park height. Thus, for the ventilation rate 10 ACH and 3.0 m carpark height the flow rate is 33,450 m^3/h, which corresponds to outflow velocity 0.516 m/s in each vent opening. Modelling details of hydrogen storage tank blowdown through TPRDs of different diameters and release directions are described in Section 4.2 below. In all simulations it was assumed that the onboard hydrogen storage tank had volume of 62.4 l and overpressure 700 bar.

Pressure-based implicit solver and the second-order upwind discretisation scheme for convective terms in all transport equations were employed. A constant time step $\Delta t = 5$ ms was used in all simulations

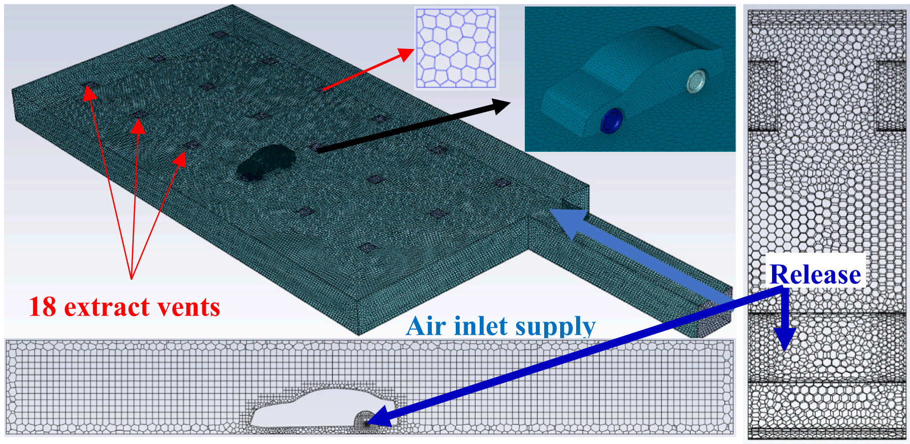

Fig. 3. Calculation domain and numerical grid. (For interpretation of the references to colour in this figure, the reader is referred to the web version of this article.)

resulting in a variable Courant–Friedrichs–Lewy (CFL) number which was maximum of 395 at the beginning of the release and decreased to 200 due to decreasing velocity at the nozzle as blowdown progressed. The described model was realised using ANSYS Fluent 2020R2 as a CFD engine.

Details of 19 numerical tests are presented in Table 1. Hydrogen releases from TPRD of diameter 0.5 mm, 0.6 mm, 0.75 mm, 1 mm and 2 mm were simulated. The effects of ventilation, release diameter and release angle, ceiling height and presence of an obstacle in a form of wall behind the vehicle were investigated. The angle of the TPRD release direction to the vertical varied in the range 0–60°. For the cases with TPRD angle 30–60° the releases were directed backwards from the vehicle. The assessed configurations are in line with the GTR #13 regulations to not direct the hydrogen gas discharge from the TPRD towards the vehicle case or wheel housing, and not “forward from the vehicle, or horizontally (parallel to road) from the back or sides of the vehicle” [22]. The FCEV was positioned close to the car park centre as shown in Fig. 3 with exception of simulations No. 12, 13 and 19, where the vehicle was in proximity of the back wall. Simulations No. 11–13, 15–17 and 19 investigated the limiting scenario of an underground parking with ceiling height 2.1 m, which is the minimum height recommended for such infrastructure [23].

Table 1
Details of numerical tests with hydrogen release and jet fire.

No.	$\varnothing_{TPRD}$, mm	ACH	Angle, °	Obstacle	Ceiling height, m	Release *
1	0.5	0	45	–	3.0	I + U
2	0.5	10	45	–	3.0	I + U
3	0.5	10	0	–	3.0	I + U
4	0.5	10	30	–	3.0	I + U
5	0.5	10	60	–	3.0	I + U
6	0.75	10	30	–	3.0	U
7	0.75	10	0	–	3.0	U
8	0.75	10	45	–	3.0	I + U
9	1.0	10	45	–	3.0	I + U
10	2.0	10	45	–	3.0	I + U
11	0.75	0	45	–	2.1	I + U
12	0.5	0	45	Wall	2.1	U
13	0.75	0	45	Wall	2.1	U
14	0.75	0	45	–	3.0	U
15	0.75	10	45	–	2.1	I + U
16	0.5	10	45	–	2.1	I
17	0.6	10	45	–	2.1	I
18	0.6	10	45	–	3	I
19	0.5	10	45	Wall	2.1	I

Note: I-ignited, U-unignited.
* means that there is no obstacle in the simulation that can be changed to N/A

4.1.2. *Ignited releases*

For simulation of ignited releases the described above problem formulation also included the Eddy Dissipation Concept (EDC) [24] as a combustion model and the Discrete Ordinate (DO) [25] radiation model. Additionally to unignited release scenarios the CFD model accounted heat transfer through the concrete car park walls. The same numerical grid and boundary conditions as per the unignited release scenario were employed.

The DO model was discretised using 5 × 5 rays and 3 × 3 pixels. The absorption coefficient for water vapour was implemented using the User Defined Function (UDF) capability of ANSYS Fluent as a dependence on temperature and water vapour partial pressure based on the data of Planck mean absorption coefficient in [26]. The proposed CFD approach has been thoroughly assessed and validated in previous works by the authors [27–29]. The numerical requirements for the grid refinement and time discretisation used in this work follow the conclusions in [27–29] used to simulate accurately experiments on hydrogen jet fires. In the described simulations the concrete wall emissivity coefficient was equal to 0.94 and emissivity coefficient of vehicle bodywork was set to 1.0 to not have reflection of radiation. The atmospheric humidity is expected to contribute to radiative heat exchange and was accounted following Chow et al. [30] who reported relative humidity in the range 40–70 % for underground car parks. In the present study, the average value of 55 % was considered for the relative humidity in air, which corresponds to a water vapour mass fraction of 0.004673 in air. The ignition of the jet was realised via patching a hot spot with temperature of 2400 K in the vicinity of the release point to initiate the reaction.

4.2. *Blowdown simulations*

The volumetric source technique [31] was applied to simulate the blowdown release for all 19 scenarios. For each selected nozzle diameter, the changing with time hydrogen mass flow rate, velocity, temperature, turbulence model parameters at the notional nozzle were modelled applying source terms in corresponding equations. The dynamics of storage pressure, mass flow rate, temperature and velocity in the notional nozzle were calculated using e-Laboratory tool “Adiabatic blowdown of storage tank” and are shown in Fig. 4. Turbulence intensity in the notional nozzle was chosen as $TI = 25\%$, turbulence length scale as $TLS = 0.07d_{not}$, where d_{not} is the diameter of the notional nozzle calculated following [13]. The part of calculation domain where the of volumetric source term is applied was modelled as a cube with the side size l_{VS} chosen in such a way that the side area was equal to the maximum notional nozzle area at the start of the release; the cube side size l_{VS} and the total volume V_{VS} for different TPRD diameters are given in Table 2. The cubic volume for source terms application was resolved using 2 × 2 × 2 cubic control volumes.

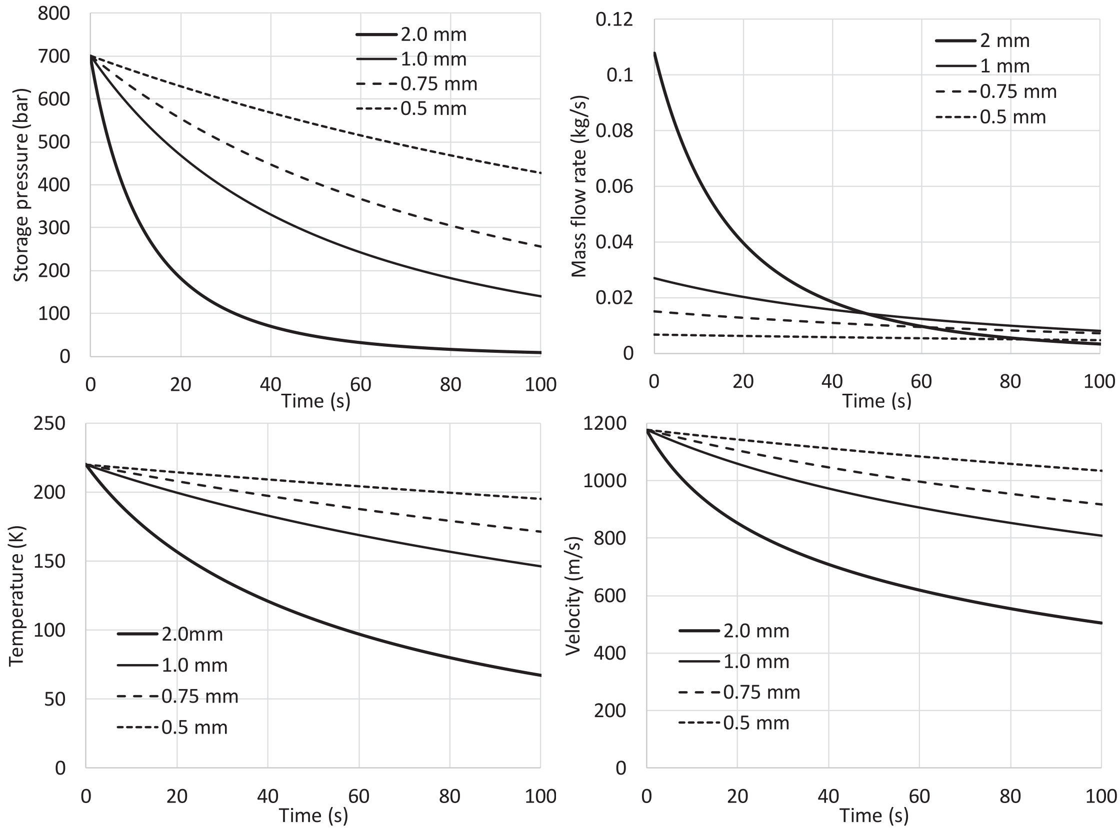

Fig. 4. Dynamics of storage pressure, mass flow rate, notional nozzle temperature and velocity during the initial stage of hydrogen tank blowdown.

Table 2
Volumetric source parameters used in CFD simulations.

$\varnothing_{TPRD}$, mm	Storage P, MPa	Storage T, K	l_{VS} side, mm	V_{VS}, m^3
0.5	70	288	7.47	$4.16{\cdot}10^{-07}$
0.6			8.96	$7.19{\cdot}10^{-07}$
0.75			11.2	$1.41{\cdot}10^{-06}$
1.0			14.9	$3.33{\cdot}10^{-06}$
2.0			29.9	$2.67{\cdot}10^{-05}$

The source terms were calculated as follows:

- mass conservation equation source term: $S_{mass} = \frac{\dot{m}_{H_2}}{V_{vs}}$,
- x-momentum (horizontal) conservation equation source term: $S_{x.mom} = \frac{u_{H_2}\cdot\dot{m}_{H_2}}{V_{vs}}\cdot sinA$, where u_{H2} is the notional nozzle velocity and A is the TPRD release direction angle to the vertical,
- y-momentum (vertical) conservation equation source term: $S_{y.mom} = -\frac{u_{H_2}\cdot\dot{m}_{H_2}}{V_{vs}}\cdot cosA$,
- z-momentum (normal to release direction) conservation equation source term: $S_{z.\ mom} = 0$,
- kinetic energy κ conservation equation source term: $S_\kappa = \frac{\kappa\cdot\dot{m}_{H_2}}{V_{vs}}$,
- dissipation energy ε source term: $S_\varepsilon = \frac{\varepsilon\cdot\dot{m}_{H_2}}{V_{vs}}$,
- energy conservation equation source term: $S_E = \frac{c_{p,H_2}\cdot(T_{H_2}-T_0)\cdot\dot{m}_{H_2}}{V_{vs}}$, where $c_{p,\ H_2}$ is the hydrogen specific heat at constant pressure, T_{H2} is the notional nozzle temperature, T_0 is the ambient temperature,
- kinetic energy: $\kappa = \frac{3}{2}(u_{H_2}\cdot TI)^2$,
- dissipation rate of turbulent kinetic energy: $\varepsilon = 0.0845^{0.75}\frac{\kappa^{1.5}}{TLS}$.

5. Results and discussion

5.1. Unignited release

5.1.1. Effect of mechanical ventilation

The simulations were performed without ventilation (0 ACH) and with ventilation rate 10 ACH to assess its effect on the formation of the flammable layer under the ceiling and estimate the hazard distance based on the distance to LFL (i.e. flammable envelope size). Fig. 5 shows flammable envelopes in the central cross section obtained in simulations for TPRD ∅0.5 and TPRD ∅0.75 mm for 3 m ceiling height, and for TPRD ∅0.75 mm for 2.1 m ceiling height; in all demonstrated cases TPRD release was directed at the angle A = 45° to the vertical. The shown snapshots are for the moments when the longest hazard distance during the blowdown release of hydrogen is observed. Fig. 5 demonstrates that there is no visible effect of mechanical ventilation on the maximum hazard distance. This is different from what was observed by Choi et al. [6] and Matsuura et al. [7]. It is thought that the obtained result is due to higher velocities of hydrogen jet compared to air velocity and the comparatively short time when the jet reaches its maximum size during the blowdown process. Fig. 5 shows as well that the flammable part of hydrogen-air jet is momentum-dominated, attached to the ground and hydrogen concentration decays below 4 % long time before it is affected by buoyancy and reaches the ceiling, thus no accumulation of hydrogen and flammable mixture formation under the ceiling is expected.

The semi-transparent blue colour contour in Fig. 5 shows the iso-surface of 4 % vol. hydrogen in the air as a maximum distance in the release direction (exact timing of the flammable envelope can be seen in Fig. 7), while the next grade of blue shows 4 % decay across the centre-plane. It can be seen that in all cases the maximum distance of flammable envelope propagation is larger than its distance in the centre-plane. This is due to the shift of TPRD location from the vehicle axis, impingement and attachment of hydrogen jet at the floor. This can also

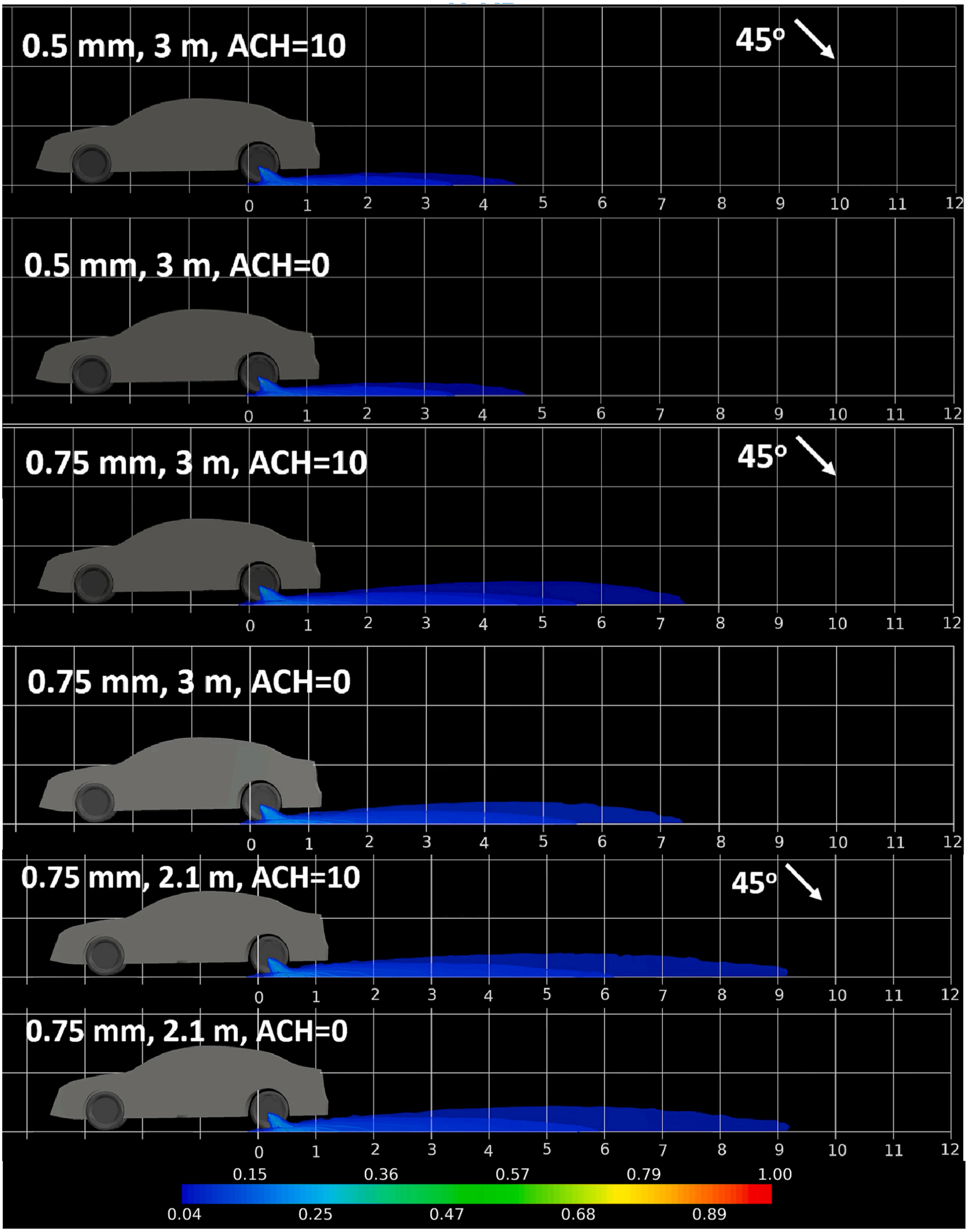

Fig. 5. Comparison of hydrogen flammable envelope with ventilation (10 ACH) versus no ventilation (0 ACH): TPRD ∅0.5 mm, A = 45°, 3.0 m ceiling (top); TPRD ∅0.75 mm, A = 45°, 3.0 m ceiling (middle); TPRD ∅0.75 mm, A = 45°, 2.1 m ceiling (bottom). (For interpretation of the references to colour in this figure, the reader is referred to the web version of this article.)

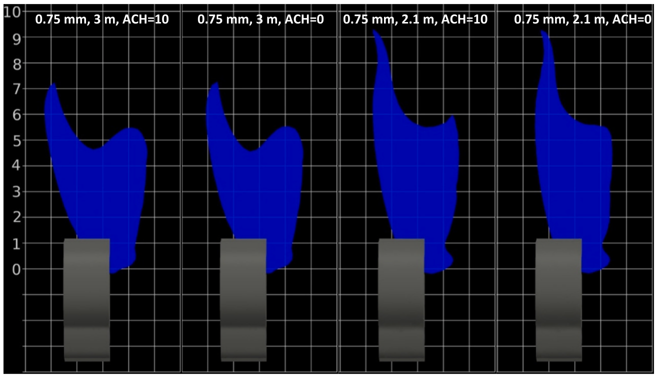

Fig. 6. Flammable envelope shape top view: TPRD ∅0.75 mm, A = 45°, 2.1 and 3 m ceiling, 0 ACH and 10 ACH at time $t = 7$ s.

be seen in Fig. 6 which shows top view of the flammable envelope for the case of TPRD ∅0.75 mm, release at the angle A = 45° to the vertical, ceiling heights 2.1 and 3.0, with and without ventilation at time $t = 7$ s. It should be noted that for the case of mechanical ventilation with 10 ACH the width of the flammable envelope is wider compared to no ventilation (0 ACH).

Fig. 7 shows dynamics of maximum horizontal distance of flammable envelope propagation from the release point in simulations No. 1–11, 14 and 15. Fig. 7 (left) for TPRD ∅0.5 mm and angle A = 45° demonstrates that the larger release angle to vertical the larger hazard distance. The maximum hazard distance is only marginally (3.5 %) decreased by the ventilation. Fig. 7 (right) shows horizontal maximum hazard distance for larger TPRD diameters in the range 0.75–2.0 mm. It reaches its maximum within 4–10 s and then gradually decreases due to blowdown. For TPRD ∅0.75 mm, A = 45° and ceiling heights 2.1 and 3.0 m the effect of ventilation is practically indistinguishable. It should be noted that in simulations the maximum flammable envelope propagation distance was achieved for TPRD ∅1.0 and ∅2.0 mm and was limited by the carpark wall, which was located in 12 m from the release point.

5.1.2. *Effect of the ceiling height*

Fig. 6 also demonstrated the effect of the ceiling height on the extension of the flammable envelopes, as shown from comparison for the same TPRD ∅0.75 mm and for 3.0 m and 2.1 m ceiling heights, both with and without ventilation. It can be seen that for the lower ceiling the largest flammable envelope propagation distance is about 2.0 m longer (25 %) which presumably is due to the different entrainment of air caused by a 30 % reduction of the height. Fig. 7 shows that this difference is reached between $t = 6.0$–6.5 s (2.1 m height) and $t = 8.0$–8.5 s (3.0 m height). The difference gradually decreases with time and stabilises at about 1.0 m (12 %) after time $t = 12$ s. As it is shown in Fig. 6 the maximum distance of flammable envelope propagation was achieved not on the jet axis, but at its periphery.

5.1.3. *Effect of TPRD release angle*

Simulations No. 2–8 (TPRD ∅0.5 mm and ∅0.75 mm, 10 ACH, ceiling height 3.0 m) were used to assess the effect of TPRD release direction, which varied between A = 0° and 60° to vertical, on the flammable envelope propagation. Fig. 8 shows the flammable envelopes at the moment they reach their maximum size in each particular simulation. For both investigated TPRD diameters the increase of the angle consistently increased the maximum hazard distance (no simulation for A = 60° and TPRD ∅0.75 mm was performed as the LFL propagation distance in this case would be even further).

Releases at A = 0° and 30° produced shorter flammable envelope distances compared to releases at A = 45° for both TPRD diameters, however they created large flammable clouds underneath the car towards the front and side passenger doors threatening passengers' evacuation in case of ignited release. Additionally, releases at angle A = 30° resulted in a thicker flammable envelope compared to A = 45° in both simulations, TPRD ∅0.5 and ∅0.75 mm.

Fig. 9 shows that releases vertically down (at angle A = 0°) are capable to form buoyant flammable clouds which can accumulate under the ceiling even with active mechanical ventilation (10 ACH).

For the above reasons only releases at the angle A = 45° will be analysed further.

5.1.4. *Effect of TPRD diameter*

Effect of TPRD diameter on flammable cloud shape is demonstrated in Fig. 10. The figure shows flammable envelopes created by releases from TPRDs ∅0.5, ∅0.75, ∅1.0 mm and ∅2.0 mm at the time $t = 6$ s. Flammable compositions for TPRD ∅0.5, ∅0.75 and ∅1.0 mm decay a long time before the jet propagation is affected by buoyancy preventing flammable cloud formation under the ceiling. At time $t = 6$ s the flammable composition from TPRD ∅2.0 mm for the considered parking area reaches the ceiling, this appears to be the most hazardous case since its flammable envelope is not only the longest one, but, after losing its momentum due to interaction with the wall, threatens with accumulation of substantial hydrogen-air cloud.

5.1.5. *Effect of obstruction in absence of ventilation (worst case)*

Simulations No. 12 and 13 (TPRD ∅0.5 and ∅0.75 mm, angle A = 45°) were performed to assess the worst-case scenario of FCEV located in a parking space next to a wall, under a low ceiling (height 2.1 m) and in absence of ventilation (0 ACH). TPRD release was directed towards the

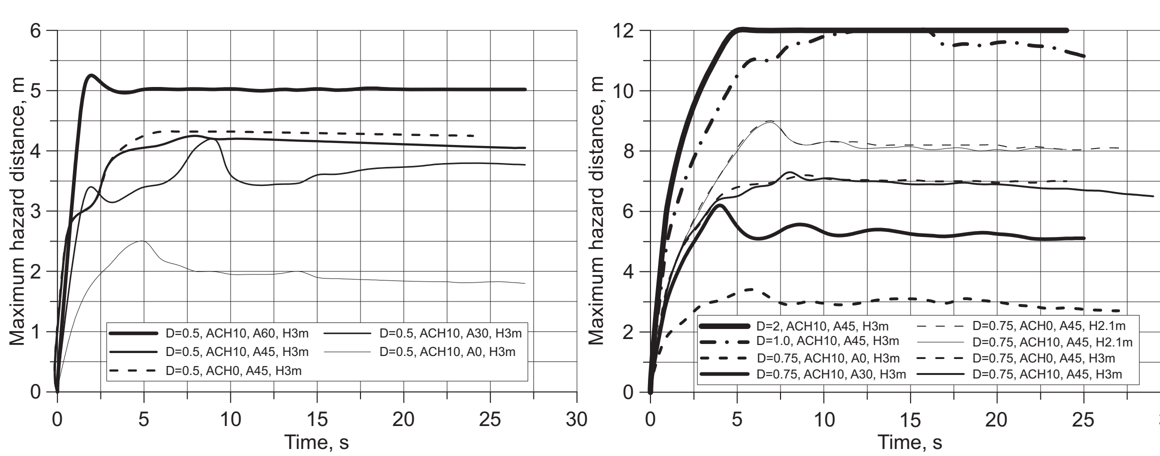

Fig. 7. Dynamics of maximum flammable envelope propagation in the presence and absence of ventilation and for different release angles. Left: TPRD ∅0.5 mm. Right: TPRD ∅0.75–2.0 mm (includes different ceiling heights; max. envelope propagation 12 m is limited by the carpark wall).

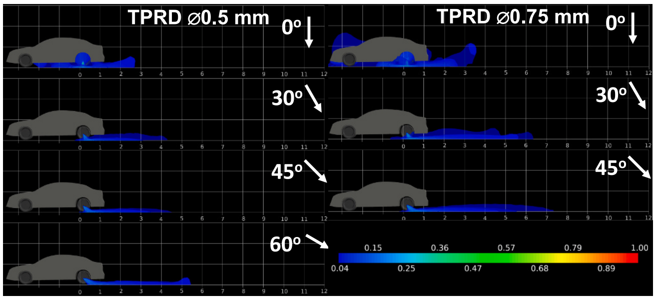

Fig. 8. Effect of release angle on the maximum extension of a flammable envelope: TPRD ∅0.5 mm (left), TPRD ∅0.75 mm (right), 3.0 m ceiling height, 10 ACH.

wall, the distance between the wall and FCEV bumper was 0.2 m. Fig. 11 shows the longest flammable hydrogen-air mixture propagation at the time $t = 8$ s for ∅0.5 and $t = 11$ s for ∅0.75 mm. Simulations demonstrate that currently the formation of flammable cloud cannot be avoided even in the case of the smallest considered TPRD ∅0.5 and ∅0.75 mm when FCEV is parked next to a wall. It is recommended to avoid parking the vehicle with TPRD directed towards the obstruction.

5.1.6. Mass of flammable hydrogen and potential overpressure hazards in case of ignition

Pressure hazards of potential hydrogen-air cloud deflagration were studied using an available analytical model for a localised mixture deflagration in a closed vessel [32]. The model is based on a number of assumptions: perfectly sealed enclosure (no openings to provide deflagration venting); localised hydrogen-air mixture occupies only portion of the enclosure, but has uniformly distributed hydrogen within the mixture at LFL 4 % vol. (which provides the largest deflagration overpressure for a given hydrogen mass); complete combustion. The analysis performed in [32] concluded that to avoid deflagration overpressure above 10 kPa, which is a typical limit for integrity of civil structures, the hydrogen inventory in the enclosure should not be larger than $m_{H2} = 2.61 \cdot 10^{-4}\ V$, where m_{H2} is the mass of hydrogen (kg) and V is the volume of the enclosure (m^3).

The studied parking has a volume of 3345 m^3. Application of the above analysis to the considered carpark means that to reach uniform across the whole parking overpressure 10 kPa the mixed with air hydrogen mass should be $m_{H2} = 2.61 \cdot 10^{-4} \cdot 3{,}345 = 0.873$ kg. In reality, the deflagration of this hydrogen mass would result in lower than 10 kPa overpressure because: (1) the parking is not perfectly sealed and has openings at least in form of extraction ventilation and entrance gate, and (2) any deviation of real mixture hydrogen content from assumed in the model uniform 4 % vol. composition (with fixed total hydrogen mass) decreases resultant overpressure.

Fig. 12 shows the dynamics of hydrogen-air cloud mass in the parking for all studied release scenarios. Fig. 12 (left) gives dynamics of hydrogen mass within the flammability limits (4–74 % vol. hydrogen). The maximum hydrogen mass reaches ca. 0.38 kg for release from the largest TPRD ∅2.0 mm, 10 ACH, release angle A = 45°. This is significantly lower than the analytical limit of 0.873 kg leading to the conclusion that deflagration of hydrogen releases from TPRD equal and lesser than ∅2.0 mm will not result in overpressures threatening structural integrity.

Releases from smaller TPRDs result in a further decrease of hydrogen mass within the flammability limits. The least flammable hydrogen mass is observed, naturally, for TPRD ∅0.5 mm (release angle A = 0°) – here maximum hydrogen mass is about 27 g, which is 14 times smaller compared to about 380 g for TPRD ∅2.0 mm (A = 45°). Increase of release angle from A = 0° to 60° for TPRD ∅0.5 mm decreases flammable hydrogen mass further down to just 4 g – nearly 7 times.

Fig. 12 (right) shows hydrogen mass in the fastest burning (and the most hazardous for overpressure generation) composition 25–35 % vol. The largest hydrogen mass of just 1.55 g was registered for release from TPRD ∅2.0 mm. This corresponds to 0.062 m^3 volume of stoichiometric hydrogen-air mixture at 29.5 % vol. hydrogen. Simulation of deflagrations of hydrogen-air mixtures resulting from TPRD releases was out of the scope of the present study but was performed within HyTunnel-CS project and reported in its deliverable D6.9 [12]. It was demonstrated that for a leak from hydrogen storage with normal working pressure (NWP) 70 MPa, reduction of TPRD diameter from ∅2.0 mm to ∅0.5 mm decreases propagation of deflagration overpressure threshold 1.35 kPa corresponding to "no-harm" limit to human life from 10.5 m to 2.6 m, making "no-harm" distance comparable to the vehicle size and is recommended as a measure to mitigate pressure effects from ignition of TPRD releases.

5.2. Ignited release

This section aims at assessing if the existing mechanical ventilation systems continue to comply with RCS requirements in case of hydrogen jet fire, particularly BS 7346-7-2013 recommendation for the system fans to operate at 300 °C for a period not less than 60 min. In order to achieve this the temperature limit of 300 °C is monitored: the ventilation system is considered inherently safe if the produced by hydrogen jet fire hot gases with temperature above 300 °C do not enter the ventilation ducts. This is a conservative assessment as the duration of hydrogen jet fires will likely be shorter than 60 min. The effect of TPRD diameter and release direction, ventilation rate and vehicle location in a car park were assessed. The results are reported in the following sections.

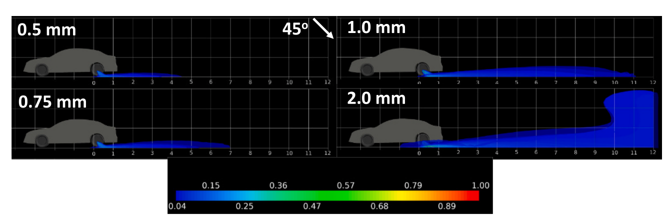

Fig. 10. Effect of TPRD diameter on flammable envelope propagation: A = 45°, 10 ACH.

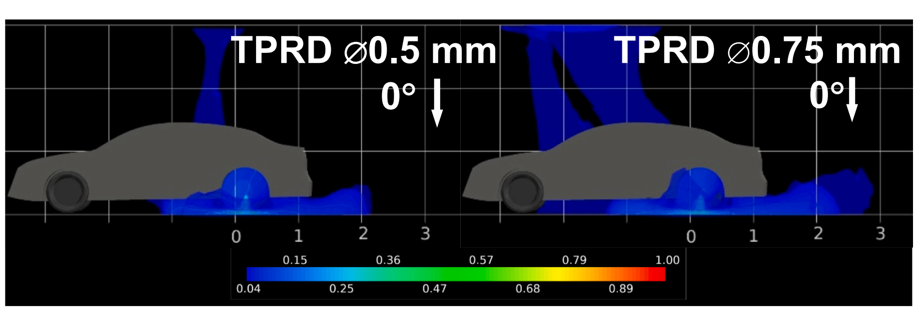

Fig. 9. Downward releases at 30 s from TPRD ∅0.5 mm (left), ∅0.75 (right), A = 0°, 10 ACH.

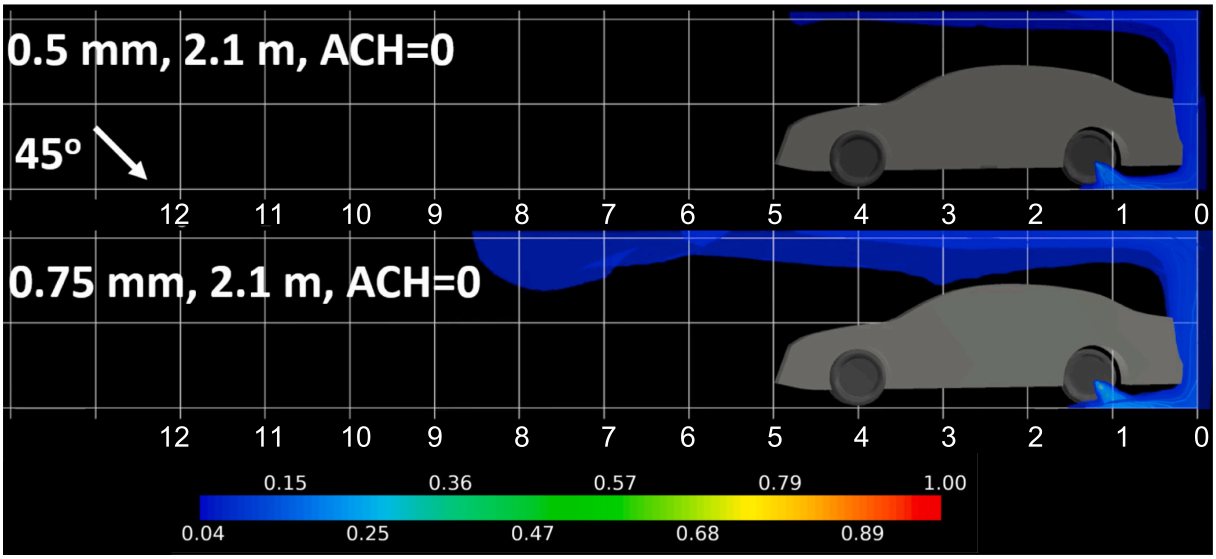

Fig. 11. Effect of obstacle on flammable cloud formation: TPRD ∅0.5 mm, $t = 8$ s (top) and ∅0.75 mm, $t = 11$ s (bottom), A = 45°, 10 ACH.

5.2.1. Effect of mechanical ventilation presence

The effect of mechanical ventilation on the combustion products cloud with temperature equal or above 573 K (300 °C limit) is shown in Fig. 13. Distribution is given for release with TPRD ∅0.5 mm, release angle A = 45° to vertical at the time $t = 16$ s, when the cloud reaches the maximum height. It could be observed that ventilation presence does not affect significantly the hot products distribution similarly to the unignited releases. Mechanical ventilation should be maintained according to current BS requirements (10 ACH).

Fig. 14 shows the dynamics of the maximum horizontal extent from the rear of a vehicle and maximum height reached by the cloud with temperature above 300 °C (573 K) threshold for TPRD ∅0.5 mm, release angle A = 45°, with and without ventilation. As it can be seen for both cases the effect of the ventilation is minimal and is comparable to the numerical accuracy.

The temperature of 70 °C (343 K) is considered as a threshold for no harm conditions for humans for any exposure duration [16]. Fig. 15 shows the dynamics of the maximum extension of the hot combustion products cloud with temperature above 70 °C from the rear of a vehicle as observed between height limits 0 and 2 m (i.e. human height) for the same simulation. The maximum peak seen at $t = 6$ s is due to momentum of hot products propagation after the initialisation of the release, which fades quickly and then expected to monotonically decrease with time as blowdown progresses.

5.2.2. Effect of TPRD release angle

Effect of TPRD release direction on thermal hazard distance was studied similar to unignited releases by simulating release angle as A = 0°, 30°, 45° and 60° to vertical. Fig. 16 shows the simulated distribution of combustion products with temperature above 300 °C at the time when the maximum height is achieved for each TPRD release direction. For the considered car park ceiling height of 3 m and TPRD ∅0.5 mm all release directions led to the hot gases temperature dissipation below 300 °C long time before buoyancy brings them to the vent openings at the ceiling, thus the ventilation system will continue to comply with the BS 7346-7-2013 standard. However, it was observed that in the case of the TPRD direction with A = 0° angle the cloud with temperature above 300 °C reaches a maximum height of 2 m, though for a short time. The hot combustion products with temperature corresponding to fatality harm criteria (300 °C, third-degree burns for 20 s exposure [16]) envelop the vehicle and may prevent escape of the occupants. For A = 30° angle, the cloud with temperature above 300 °C reaches a maximum height of 2.1 m for a short time. For both A = 45° and 60° release angles the hot gases with temperature above 300 °C do not reach 2 m height. A further analysis has been conducted on hazard distances for people, according to the "no-harm" criteria 70 °C for any exposure duration [16]. It was observed that the "no-harm" distance from the vehicle is the lowest for the TPRD release angle A = 0°. However, the hot combustion products with the temperature reaching fatality harm level 300 °C surround the vehicle in this case and may prevent escape of the occupants. For the release angle A = 30° the "no-harm" distance is lower than 5 m, but as mentioned earlier the cloud with temperature above 300 °C would reach the carpark ceiling if its height is 2.1 m. For the TPRD release angle A = 45° the "no-harm" distance is calculated as 6.2 m, which is lower than distance for release with A = 60° angle. It appears that the TPRD release angle A = 45° represents the best choice in terms of minimal harm criteria for people and the hot gases cloud not preventing operation of mechanical ventilation system compliant with BS 7346-7-2013 standard. Only this A = 45° release direction will be used for further analysis of TPRD diameter effect.

Fig. 17 presents the dynamics of the maximum height and horizontal distance from the rear of a vehicle reached by the hot combustion products cloud with temperature equal or above 300 °C for different TPRD release angles. Fig. 17 (left) shows the maximum extent of the hot combustion products with temperature above 300 °C in horizontal direction from the back of the vehicle. It can be observed that the maximum horizontal distance extends with the increase of the TPRD angle, which may lead to higher risk of potential secondary fires even if minimising hazards for self-evacuation of occupants from the vehicle. Also from Fig. 17, it can be concluded that a TPRD with release direction A = 45° represents the best option to ease the self-evacuation of the vehicle's occupants and reduce hazard distances in both vertical and horizontal directions. Fig. 17 (right) shows the relationship between the release angle and the maximum height at which the damaging for ventilation system temperature level 300 °C is reached (keeping in mind that it cannot be larger than the height of the carpark ceiling, i.e. 3.0 m). For the release angle A = 0° the ventilation damage may occur at a maximum height of 2.0 m, although only for a short time. However, it is noted from Fig. 16 that the hot combustion products with a temperature corresponding to "fatality" harm criteria envelop the vehicle, which may prevent the escape of the passengers. This suggests that even if the damage level is not reached at the ceiling of 3.0 m height, the hot combustion products may still pose a serious threat to the safety of self-evacuation of occupants of the car park. For the release angle A = 30° the damaging temperature level reaches the maximum height of 2.1 m, even though for a short time (similar to A = 0° angle). For angles of 45° and 60°, the damaging temperature level does not reach height 2.0 m.

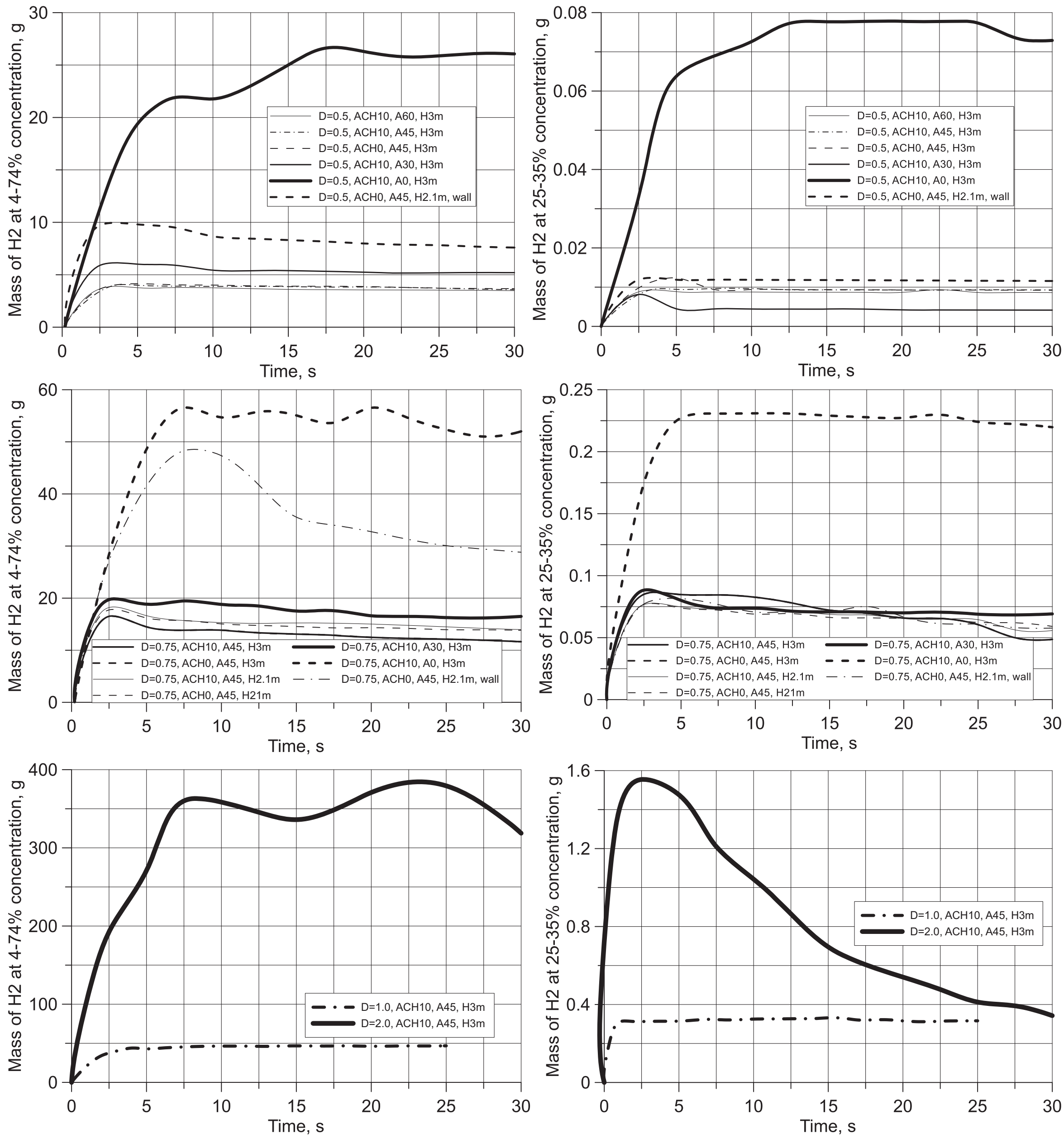

Fig. 12. Dynamics of flammable mass of hydrogen: within flammability limits 4–74 % vol. (left), within fastest burning composition 25–35 % vol. (right); TPRD ∅0.5 mm (top), ∅0.75 mm (middle), ∅1.0 mm and ∅2.0 mm (bottom).

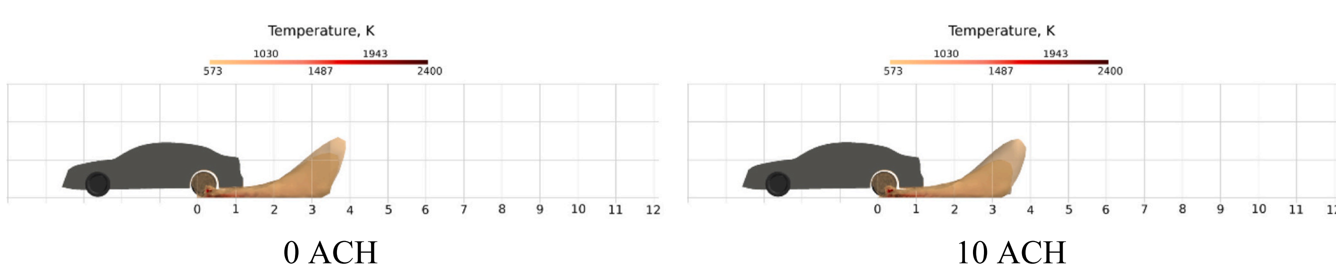

Fig. 13. Effect of mechanical ventilation (10 ACH) versus no ventilation (0 ACH) on combustion products cloud with temperature above 300 °C: TPRD ∅0.5 mm, 3.0 m ceiling height, A = 45°, time t = 16 s.

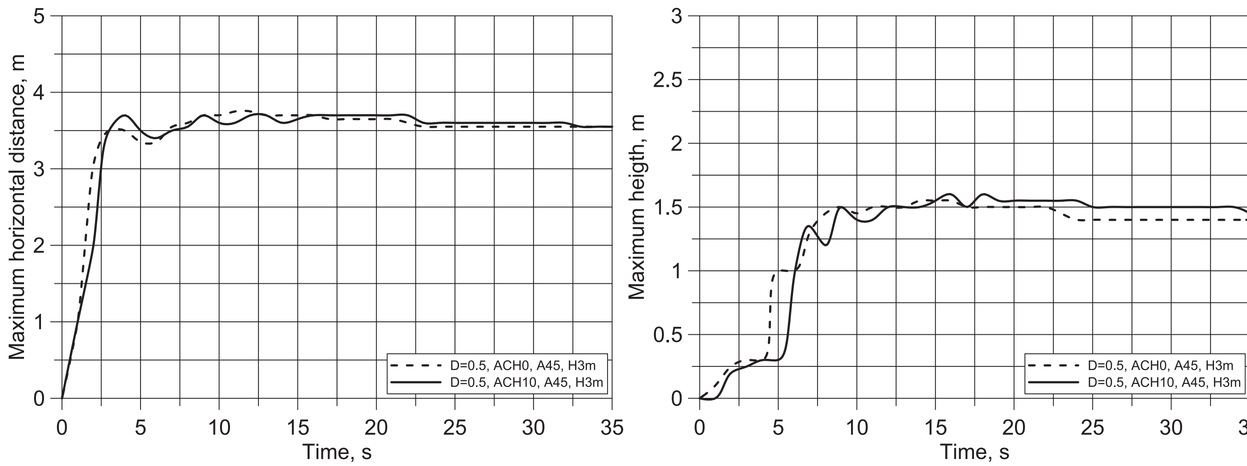

Fig. 14. Maximum horizontal extent from the rear of a vehicle (left) and maximum height (right) reached by the combustion products cloud with temperature above 300 °C: TPRD ∅0.5 mm, 3.0 m ceiling height, A = 45°.

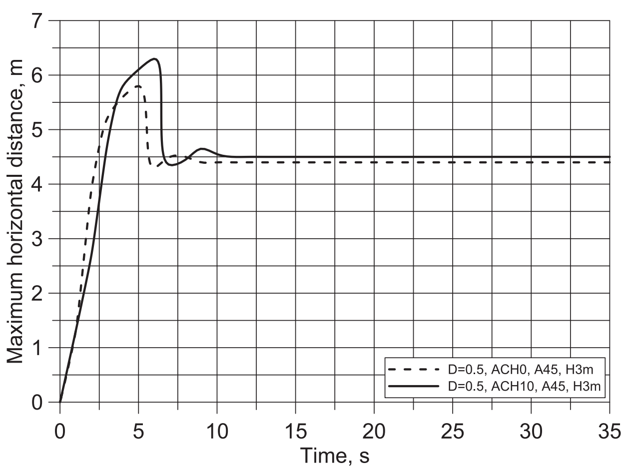

Fig. 15. Maximum horizontal distance from the rear of a vehicle reached by the combustion products cloud with temperature above 70 °C as observed between height limits 0 and 2 m: TPRD ∅0.5 mm, 3.0 m ceiling height, A = 45°.

5.2.3. Effect of TPRD diameter

The effect of a TPRD diameter on the size of hot gases cloud and safe operation of mechanical ventilation system compliant with BS 7346-7-2013 standard has been assessed in the range ∅0.5–∅2.0 mm. Fig. 18 shows the distributions of the cloud with temperature above 300 °C at the time of maximum height of the cloud for each case. It can be observed that for TPRD ∅0.5 mm the cloud with temperature above 300 °C reaches the maximum height 1.6 m and does not reach the ceiling. For a TPRD ∅0.6 mm the cloud above 300 °C reaches a 2.5 m height and does not reach ceiling either. In simulations with a TPRD ∅0.6 mm and the ceiling height of 2.1 m the temperature above 300 °C reaches the ceiling, which could undermine operation of mechanical ventilation system and carpark safety (the case is not shown in Fig. 18). For releases with both TPRD ∅0.75 and ∅1.0 mm the temperature above 300 °C reaches the ceiling within 8 s. This time is decreased to 5 s when a TPRD ∅2.0 mm is employed. In this case the hot products cloud reaches the wall at approximately 12 m behind the rear of the vehicle. The “no-harm” distances from the back of the vehicle are below 6.5 m for TPRD ∅0.5–∅0.6 mm, whereas this reaches the wall of the car park at 12 m behind the vehicle for TPRD ∅0.75–∅1.0 mm.

The results of the numerical simulations are in agreement with the observations in [33] on naturally ventilated covered car park with dimensions $L \times H \times W = 30 \times 28.4 \times 2.6$ m. The downward direction of the jet fire was seen to significantly decrease the dangerous zone for the

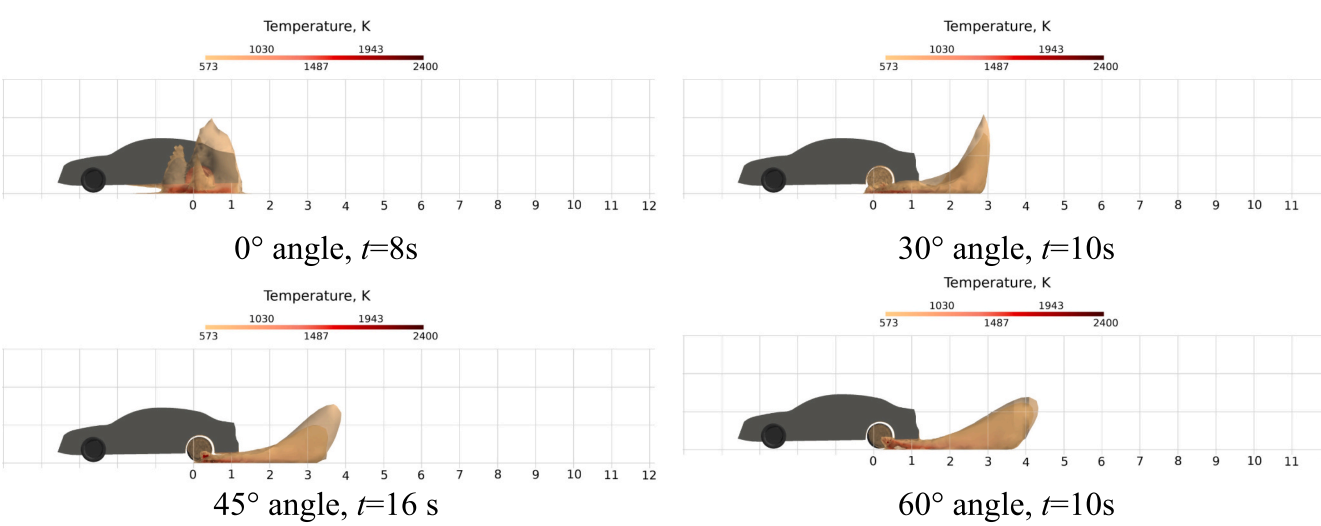

Fig. 16. Effect of TPRD release angle to vertical on the combustion products cloud with temperature above 300 °C for TPRD ∅0.5 mm: 3.0 m ceiling height, 10 ACH.

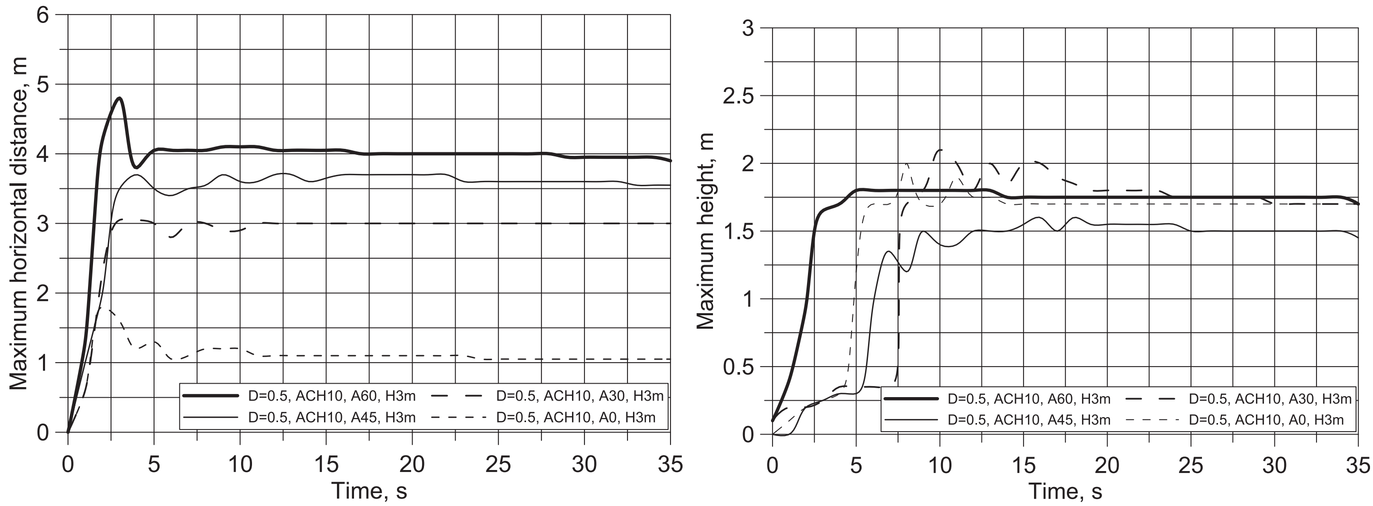

Fig. 17. Maximum horizontal distance from the rear of a vehicle (left) and maximum height (right) reached by the combustion products cloud with temperature above 300 °C for various TPRD angles: TPRD ∅0.5 mm, 10 ACH.

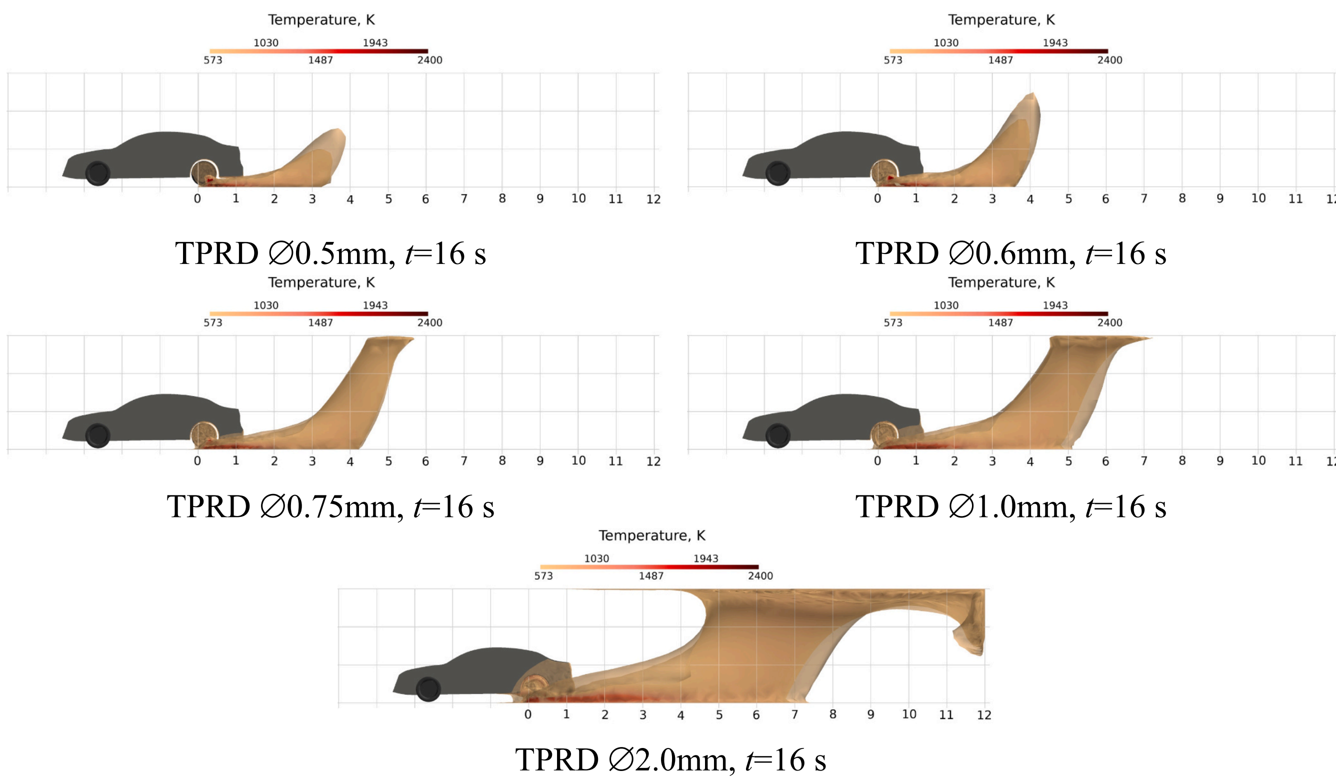

Fig. 18. Effect of TPRD diameter on the combustion products cloud with temperature above 300 °C: A = 45°, 3.0 m ceiling height, 10 ACH.

ventilation system. In present study for the TPRD ∅2.0 mm release the hot cloud with temperature above 300 °C yet reached the ceiling for release directions at A = 0°, 30° and 45°. On the other hand, the TPRD ∅0.5 mm and release direction A = 45° did not produce the dangerous cloud at the ceiling during tank blowdown duration, e.g. in the study [33] duration of blowdown for a 117 l tank with initial pressure 70 MPa was 1 h 40 min. It should be remarked that natural ventilation may provide a lower amount of fresh air compared to mechanical ventilation.

Fig. 19 (left) depicts the maximum horizontal distance from the rear of a vehicle for the combustion products cloud with temperature above the 300 °C threshold. The graph provides insight into the potential danger posed by the hot combustion products and their impact on the ventilation system safety. As can be seen from right figure with TPRD ∅0.5 mm, the temperature level damaging ventilation is not reached under the 3.0 m high ceiling and temperature 300 °C reaches maximum height 1.6 m only. With TPRD ∅0.6 mm the damaging temperature level is not reached under the ceiling for a car park height of 3.0 m, however, temperature threshold 300 °C is reached at 2.5 m height, which could undermine safety for car parks with the height below this value. With TPRD ∅0.75–∅1.0 mm the damage level under the ceiling is reached within 8 s.

As can be seen in Fig. 20 for the TPRD ∅0.5–∅0.6 mm, the maximum "no-harm" distance from the rear of a vehicle is achieved at about 6.5 m. This hazard distance from the vehicle should be maintained for any

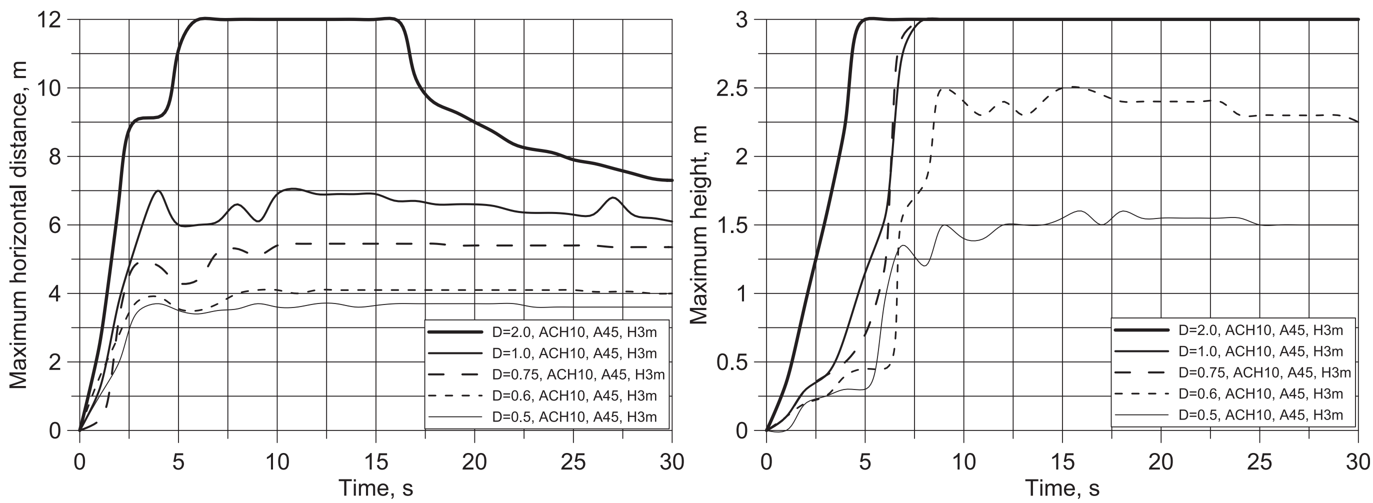

Fig. 19. Maximum horizontal distance from the rear of a vehicle (left) and maximum height (right) reached by combustion products cloud with temperature above 300 °C for various TPRD diameters: A = 45°, 10 ACH.

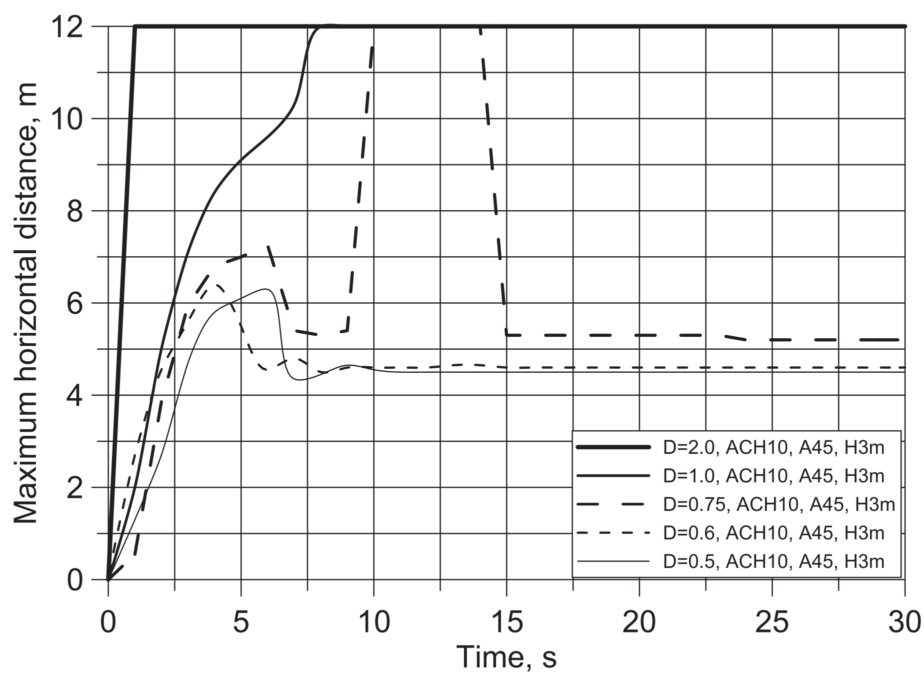

Fig. 20. Maximum horizontal distance from the rear of a vehicle reached by the combustion products cloud with temperature above 70 °C as observed between height limits 0 and 2 m for various TPRD diameters: A = 45°, 10 ACH.

pedestrians to prevent any potential harm. On the other hand, the TPRD ∅0.75–∅1.0 mm is observed to provide harmful conditions up to the wall of the car park located behind the vehicle at 12 m distance. However, it should be remarked that reduction of a TPRD diameter for the same tank volume elongates the time required for the blowdown of the pressurised storage system. In the event of tank exposure to a fire, it should be ensured that the storage tank fire resistance rating is still sufficient for the given TPRD diameter to blowdown the tank before its catastrophic rupture. One of the promising technologies is Leak-no-burst (LNB) safety technology for Type IV tanks, which can prevent catastrophic tank rupture even in the event of a fire even with a non-functioning TPRD [34]. Another inherently safer engineering solution to ensure tank integrity in a fire is tank-TPRD design as a system, which prevents conventional composite tanks rupture with TPRD orifices as small as ∅0.5 mm [35].

6. Safety strategies and recommendations

The results of the performed numerical analysis are used to formulate safety strategies and recommendations to underpin the inherently safer introduction of FCEV into underground infrastructure. The criteria employed for the assessment of the proposed safety strategies include the compliance to current RCS ventilation requirements in underground carparks and the facilitation of self-evacuation or rescue from the FCEV. It is worth mentioning that some of the listed recommendations on optimum TPRD diameters and angles are based the specific case considered in this paper: downwards hydrogen jets directed backwards a FCEV in an underground car park of dimensions 45 × 3 × 23 m, with an onboard hydrogen storage tank volume of 62.4 l and NWP 700 bar.

- The general safety strategy for unignited releases in underground parking is to eliminate the formation of flammable cloud under the ceiling.
- For the upward releases, the similarity law can be used to calculate at what TPRD size the hydrogen jet will decay below 4 % vol. (LFL) before reaching the ceiling.
- The ventilation rate required by RCS for carparks does not affect the hydrogen flammable clouds formed by releases from TPRD ∅0.5–∅0.75 mm.
- TPRD release direction at the angle A = 45° is deemed to be the overall best safety solution. Releases at the angle A = 0° generate buoyant hydrogen-air plume forming a flammable layer under the ceiling. Releases at the angle A = 0° and 30° provide mixture propagation towards the front and rear wheels, which, if ignited, will contradict to RCS requirements for FCEV.
- Releases from TPRD ∅0.5 and ∅0.75 mm do not result in a flammable layer formation under the carpark ceiling for the considered range of ceiling heights (2.1–3.0 m) and ventilation rates from 0 ACH (no ventilation) to 10 ACH (required mechanical ventilation rate in case of fire).
- Releases from TPRDs above ∅0.75 mm have the potential to create a flammable layer, especially in the absence of mechanical ventilation.
- Releases from TPRD towards obstacles tend to prohibit hydrogen mixing with air and promote accumulation of a flammable cloud; it should be recommended not to park FCEV with TPRD directed towards any obstruction.
- The use of analytical models for analysis of mechanical ventilation effect on hydrogen propagation from onboard storage releases deem to suffer loss of accuracy due to transient and highly non-uniform hydrogen distribution. This is particularly pronounced for enclosures with large volume and complex geometries. The use of more accurate methods capable to resolve spatial and temporal hydrogen dynamics like CFD should be considered for these problems.
- The strategy for preventing hot combustion products with temperature above 300 °C from reaching the underground parking ceiling will ensure FCEV compatibility with current RCS requirement for carpark mechanical ventilation to operate at least at 300 °C for 60 min. For vertical hydrogen jet fires oriented upward the dimensionless flame length correlation can be used to determine the TPRD size which will correspond to the hot products temperature dropping below 300 °C before reaching the ceiling.
- Ventilation does not significantly affect the distribution of hot combustion products and the associated hazard distances for TPRD ∅0.5 mm. This conclusion is consistent with studies on unignited jets, where it was found that the ventilation did not impact hydrogen flammable clouds formed by releases from TPRD ∅0.5–∅0.75 mm. Mechanical ventilation should be maintained according to current BS requirements (10 ACH).
- A release angle of 45° through a TPRD ∅0.5 mm is recommended to not obstruct the vehicle evacuation and reduce the hot combustion products height compared to angles 0–30°, and to reduce hazard distances compared to angle 60°. Ignited releases at an angle of 0° may obstruct self-evacuation and rescue operations from the vehicle. For release angles below 30° the formation of hot products with a temperature of 300 °C at a height of 2.0 m is observed. This height is comparable to the minimum height of 2.1 m found for underground parking.
- A release with angle 45° and TPRD ∅0.5 mm is found to comply with RCS requirements to mechanical ventilation systems when underground car parks height is 2.1–3.0 m. TPRD ∅0.6 mm is seen to comply with the requirements for a car park height of 3.0 m, however, it could pose a safety risk for car parks with a height of 2.1 m. The no-harm distance from the rear of the vehicle is similar to the case of TPRD ∅0.5 mm.
- Larger TPRDs ∅0.75–∅1.0 mm are found to result in hot products temperature above 300 °C at the ceiling height 3.0 m, which is above RCS requirement for carpark mechanical ventilation fans and may compromise their operation and carpark safety. The TPRD dimensions for jet fires are more restrictive than for unignited releases. Numerical modelling of unignited hydrogen releases shows that TPRD up to ∅0.75 mm does not result in a flammable layer formation under the car park ceiling for the considered range of ceiling heights (2.1–3.0 m).
- It should be noted that the damage criterion for ventilation system used in this study is conservative and that jet fires are expected to have a much shorter duration compared to the required resistance time for the ventilation system's fans (at least 60 min) and duration of a general car fire.
- The rupture of the onboard storage tanks should be prevented at all costs. It shall be ensured that a given design and diameter of a TPRD is assessed against the fire resistance rating of the hydrogen storage tank to exclude the eventuality of catastrophic rupture of the high-pressure equipment prior to the complete emptying of the tank.

7. Conclusions

The *originality* of the performed research is in conducting for the first time analysis of hydrogen release and dispersion and ignited jet fire from a realistic high-pressure hydrogen tank TPRD in a real underground parking taking into account the effect of release direction, angle, ceiling height and ventilation. Safety strategy based on similarity law for concentration decay along hydrogen jet axis and allowing to exclude flammable mixture formation under car parking ceiling by limiting TPRD diameter is demonstrated for vertical release direction. The dimensionless flame length correlation can be used to assess the distances to hazardous temperature levels for upwards vertical hydrogen jet fires in an underground car park. The series of 19 CFD simulations of unignited and ignited blowdown releases taking into account realistic vehicle and car parking geometry with and without account of mechanical ventilation in underground parking is performed providing detailed information on hydrogen-air mixture and hot combustion products dynamics.

The *rigour* of this work is in the consistent and detailed analysis across the whole range of potential TPRD design parameters (diameter, release direction), realistic carpark geometries (heights, space), ventilation rates (from no ventilation, 0 ACH, up to regulated 10 ACH).

The *significance* of this study is in demonstration of the proper choice of TPRD angle and diameter deemed to satisfy safety requirements in case of accidental hydrogen release and jet fire in underground carpark which mechanical ventilation is compliant with currently existing RCS. The fact enables the use of currently existing parking and underground infrastructure with the new generation of FCEV.

It should be noted that any recommendation associated with the mitigation of potential hazards by decreasing TPRD diameter shall ensure that the storage tank fire resistance rating is still sufficient to exclude catastrophic rupture of high-pressure equipment prior to a full emptying of the tank.

The above discussion has provided a valuable contribution to the recommendations to regulations, codes and standards (RCS) related to dealing with unignited and ignited hydrogen releases in confined spaces in HyTunnel-CS project deliverable D6.9 "Recommendations for inherently safer use of hydrogen vehicles in underground traffic systems".

Declaration of competing interest

The authors declare that they have no known competing financial interests or personal relationships that could have appeared to influence the work reported in this paper.

Data availability

Data will be made available on request.

Acknowledgements

The authors are grateful to Engineering and Physical Sciences Research Council (EPSRC) of the UK for funding this work through SUPERGEN Hydrogen and Fuel Cell Hub project (EP/P024807/1) and Kelvin-2 (EP/T022175/1), and the HyTunnel-CS, SH2APED and HyLICAL projects have received funding from the FCH JU (now Clean Hydrogen Partnership) under grant agreements No. 826193, No. 101007182 and No. 101101461. This Joint Undertaking receives support from the European Union's Horizon 2020 research and innovation programme, Hydrogen Europe and Hydrogen Europe Research.

References

[1] IEC 60079-10-1. International Electrotechnical Commission IEC 60079-10-1, Explosive Atmospheres - Part 10-1: Classification of Areas - Explosive Gas Atmospheres, 2015.
[2] NFPA 2, National Fire Protection Association NFPA 2. Hydrogen Technologies Code, 2011.
[3] ISO/DIS 19880-1, 19880-1 TI Organization for Standardization I. Gaseous Hydrogen – Fuelling Stations, Part 1: General Requirements. 2018, 2018.
[4] British Standard Institution BS 7346-7:2013, Components for Smoke and Heat Control Systems – Part 7: Code of Practice on Functional Recommendations and Calculation Methods for Smoke and Heat Control Systems for Covered Car Parks, 2013.
[5] P. Middha, D. Engel, O.R. Hansen, Can the addition of hydrogen to natural gas reduce the explosion risk? Int. J. Hydrog. Energy 36 (2011) 2628–2636, https://doi.org/10.1016/j.ijhydene.2010.04.132.
[6] J. Choi, N. Hur, S. Kang, E. Lee, K. Lee, A CFD simulation of hydrogen dispersion for the hydrogen leakage from a fuel cell vehicle in an underground parking garage, Int. J. Hydrog. Energy (2013) 38.
[7] K. Matsuura, M. Nakano, J. Ishimoto, Forced ventilation for sensing-based risk mitigation of leaking hydrogen in a partially open space, Int. J. Hydrog. Energy 35 (2010) 4776–4786, https://doi.org/10.1016/j.ijhydene.2010.02.068.
[8] V. Molkov, V. Shentsov, J. Quintiere, Passive ventilation of a sustained gaseous release in an enclosure with one vent, Int. J. Hydrog. Energy 39 (2014) 8158–8168, https://doi.org/10.1016/j.ijhydene.2014.03.069.
[9] B. Cariteau, I. Tkatschenko, Experimental study of the effects of vent geometry on the dispersion of a buoyant gas in a small enclosure, Int. J. Hydrog. Energy 38 (2013) 8030–8038, https://doi.org/10.1016/j.ijhydene.2013.03.100.
[10] P. Adams, A. Bengaouer, B. Cariteau, V. Molkov, A.G. Venetsanos, Allowable hydrogen permeation rate from road vehicles, Int. J. Hydrog. Energy 36 (2011) 2742–2749, https://doi.org/10.1016/j.ijhydene.2010.04.161.
[11] A.W. Lach, A.V. Gaathaug, Effect of mechanical ventilation on accidental hydrogen releases—large-scale experiments, Energies 14 (2021) 3008, https://doi.org/10.3390/en14113008.
[12] HyTunnel-CS D6.9, Recommendations for Inherently Safer Use of Hydrogen Vehicles in Underground Traffic Systems, 2022.
[13] V. Molkov, Fundamentals of hydrogen safety engineering. bookboon.com, 2012 free download online book.
[14] e-Laboratory of Hydrogen Safety n.d. https://elab.hysafer.ulster.ac.uk/ (accessed August 11, 2020).
[15] Net-Tools. Development of e-Tools to support education and training related to hydrogen und fuel cells technologies n.d. https://www.h2fc-net.eu/ (accessed August 11, 2020).
[16] J. LaChance, Analyses to support development of risk-informed separation distances for hydrogen codes and standards, in: 6th ISCARW, Belfast, 2010.
[17] V. Molkov, J.B. Saffers, Hydrogen jet flames, Int. J. Hydrog. Energy 38 (2013) 8141–8158.
[18] ArcelorMittal. Underground Car Parks n.d.
[19] T.-H. Shih, W.W. Liou, A. Shabbir, Z. Yang, J. Zhu, A new k-ϵ eddy viscosity model for high Reynolds number turbulent flows, Comput. Fluids 24 (1995) 227–238, https://doi.org/10.1016/0045-7930(94)00032-T.
[20] Z. Li, D. Makarov, J. Keenan, V. Molkov, CFD study of the unignited and ignited hydrogen releases from trpd under a fuel cell car, in: 6st Int. Conf. Hydrog. Saf., Vol. 131, Yokohama, Japan, 2015.
[21] S.G. Giannissi, I.C. Tolias, D. Melideo, D. Baraldi, V. Shentsov, D. Makarov, et al., On the CFD modelling of hydrogen dispersion at low-Reynolds number release in closed facility, Int. J. Hydrog. Energy 46 (2021) 29745–29761, https://doi.org/10.1016/j.ijhydene.2020.09.078.
[22] United Nations Economic Commission for Europe, Global technical regulation on hydrogen and fuel cell vehicles, in: Addendum 13: Global Technical Regulation No. 13. Global Registry, Global Registry: UNECE, 2013.
[23] IStructE, Design Recommendations for Multi-Storey and Underground Car Parks, 3rd ed., Institution of Structural Engineers, London, 2002.
[24] B.F. Magnussen, On the Structure of Turbulence and a Generalized Eddy Dissipation Concept for Chemical Reactions in Turbulent Flow, 1981.
[25] J.Y. Murthy, S.R. Mathur, Finite volume method for radiative heat transfer using unstructured meshes, J. Thermophys. Heat Transf. 12 (1998) 313–321, https://doi.org/10.2514/2.6363.
[26] G.L. Hubbard, C.L. Tien, Infrared mean absorption coefficients of luminous flames and smoke, J. Heat Transf. 100 (1978) 235–239, https://doi.org/10.1115/1.3450788.
[27] D.M.C. Cirrone, D. Makarov, V. Molkov, Thermal radiation from cryogenic hydrogen jet fires, Int. J. Hydrog. Energy 44 (2019) 8874–8885, https://doi.org/10.1016/j.ijhydene.2018.08.107.
[28] D.M.C. Cirrone, D. Makarov, V. Molkov, Simulation of thermal hazards from hydrogen under-expanded jet fire, Int. J. Hydrog. Energy 44 (2019) 8886–8892, https://doi.org/10.1016/j.ijhydene.2018.08.106.
[29] D. Cirrone, D. Makarov, M. Kuznetsov, A. Friedrich, V. Molkov, Effect of heat transfer through the release pipe on simulations of cryogenic hydrogen jet fires and hazard distances, Int. J. Hydrog. Energy 47 (2022) 21596–21611, https://doi.org/10.1016/j.ijhydene.2022.04.276.
[30] W.K. Chow, L.T. Wong, W.Y. Fung, Field study on the indoor thermal environment and carbon monoxide levels in a large underground car park, Tunn. Undergr. Space Technol. 11 (1996) 333–343, https://doi.org/10.1016/0886-7798(96)00025-9.
[31] V. Molkov, D. Makarov, M. Bragin, Physics and modelling of under-expanded jets and hydrogen dispersion in atmosphere, in: Proc. 24th Int. Conf. Interact. Intense Energy Fluxes Matter, Elbrus, Chernogolovka, 2009, pp. 143–145.
[32] D. Makarov, P. Hooker, M. Kuznetsov, V. Molkov, Deflagrations of localised homogeneous and inhomogeneous hydrogen-air mixtures in enclosures, Int. J. Hydrog. Energy 43 (2018) 9848–9869, https://doi.org/10.1016/j.ijhydene.2018.03.159.
[33] H. Hussein, S. Brennan, V. Molkov, Dispersion of hydrogen release in a naturally ventilated covered car park, Int. J. Hydrog. Energy 45 (2020) 23882–23897, https://doi.org/10.1016/j.ijhydene.2020.06.194.
[34] V. Molkov, D. Makarov, S. Kashkarov, European Patent Application No 18706224.5 "Composite Vessel for Hydrogen Storage", 2019.
[35] V. Molkov, M. Dadashzadeh, S. Kashkarov, D. Makarov, Performance of hydrogen storage tank with TPRD in an engulfing fire, Int. J. Hydrog. Energy 46 (2021) 36581–36597, https://doi.org/10.1016/j.ijhydene.2021.08.128.